Cell Reports, Volume *42*

Supplemental information

TRIB2 safeguards naive T cell homeostasis during aging

Wenqiang Cao, Ines Sturmlechner, Huimin Zhang, Jun Jin, Bin Hu, Rohit R. Jadhav, Fengqin Fang, Cornelia M. Weyand, and Jörg J. Goronzy

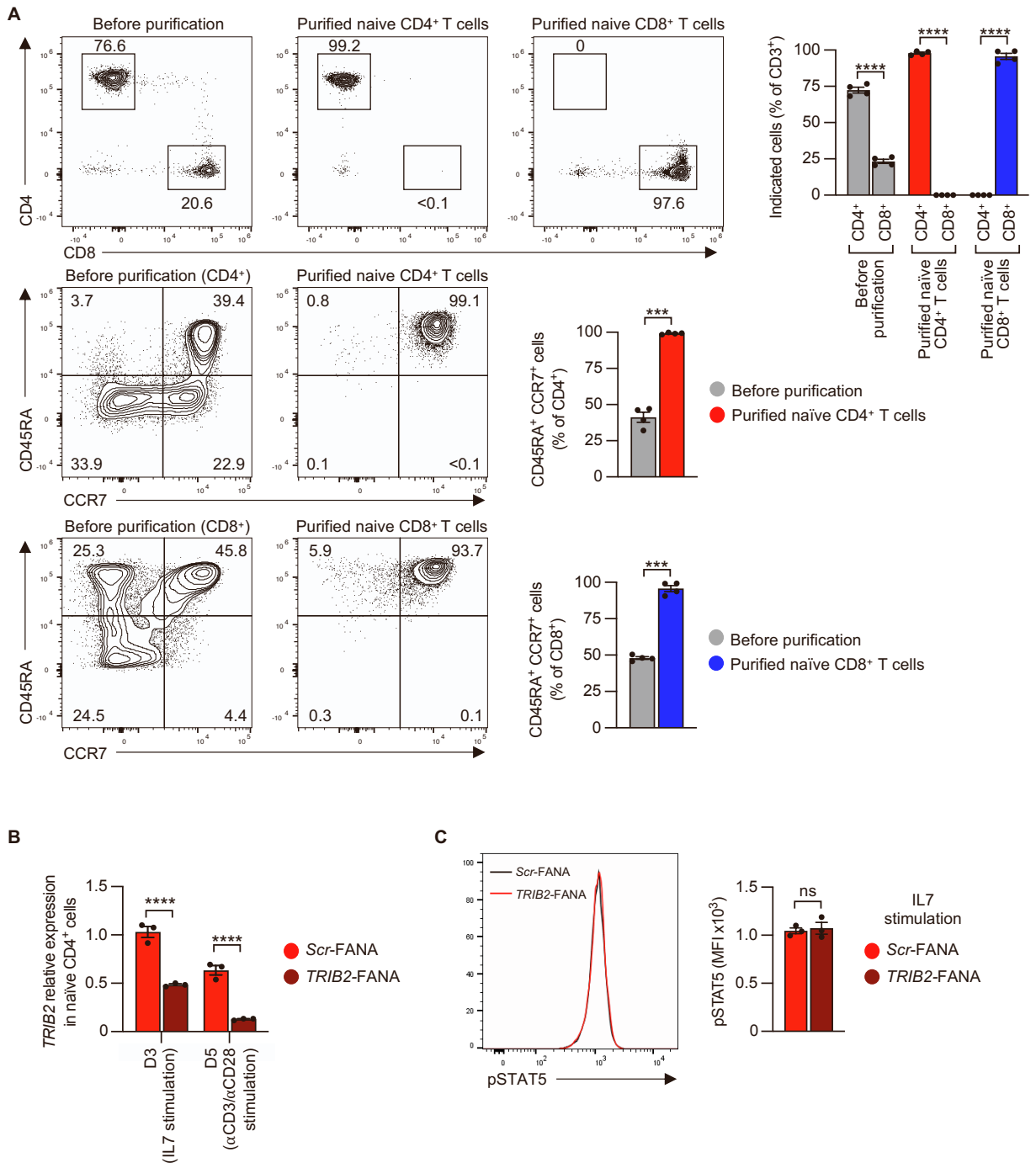

Figure S1, related to Figures 1 and 2. Influence of TRIB2 on IL7-induced signaling in naïve CD4⁺ T cells. (A) Purification of naïve CD4⁺ or naïve CD8⁺ T cells from human peripheral blood by MACS (see STAR Methods). Representative contour plots and quantitation of CD4⁺ or CD8⁺ cells among CD3⁺ T cells (top) and proportion of naïve (CD45RA⁺ CCR7⁺) cells within CD4⁺ or CD8⁺ T cells (bottom) as measured by flow

cytometry. **(B)** *TRIB2* knockdown efficiency by *TRIB2*-FANA-ASO after IL7 or anti-CD3/anti-CD28 stimulation of purified human naïve $CD4^+$ T cells. **(C)** Representative flow cytometry blots and quantification of phospho-STAT5 levels in human naïve $CD4^+$ T cells 3 days after stimulation with 50ng/ml IL7 and plate-bound anti-CD28 antibody (2 µg/ml) and incubation with *TRIB2*-targetting or scrambled (*Scr*) FANA-ASO. Results are shown as mean ± SEM (A to C). All datapoints represent distinct biological replicates. Results are from 1 experiment (A, C), or 3 experiments (B). Data were compared by two-way ANOVA with post-hoc Šídák test (A top, B) or two-tailed, paired *t*-tests (A bottom, C). ***$P \leq 0.001$, ****$P \leq 0.0001$. ns, not significant.

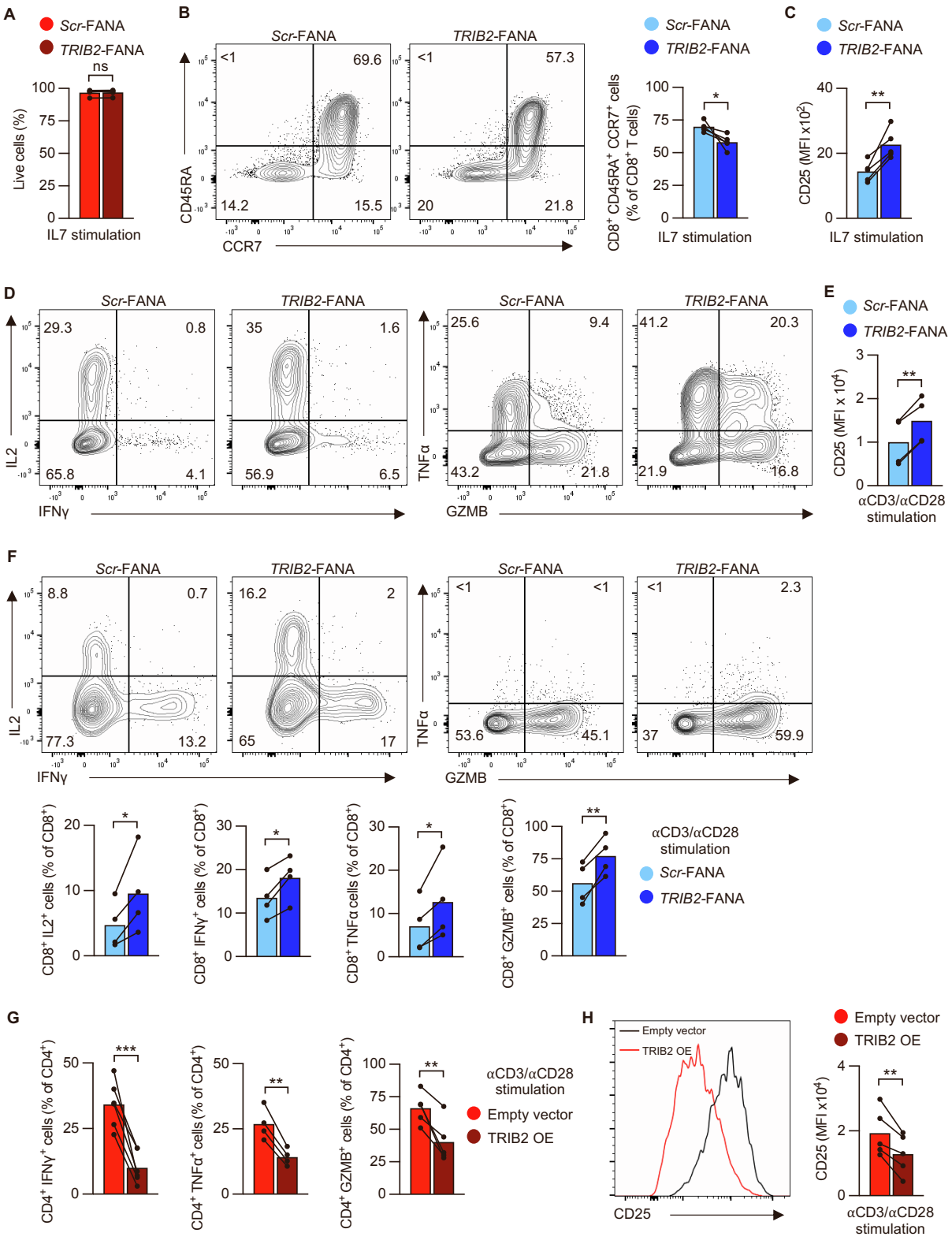

Figure S2, related to Figure 3. *TRIB2*-deficient T cells are prone to differentiation.

(A) Proportion of live human CD4⁺ T cells after FANA-ASO mediated *TRIB2* knockdown

as measured by exclusion of the viability dye in flow cytometry experiments. Data correspond to experiment shown in Figure 3A and 3B. **(B)** Representative contour plots and frequencies of naïve CD45RA$^+$ CCR7$^+$ CD8$^+$ T cells after FANA-ASO-mediated *TRIB2* knockdown. Purified human naïve CD8$^+$ T cells were cultured with 50 ng/ml IL7 and plate-bound anti-CD28 antibody (2 µg/ml) in the presence of indicated FANA-ASO for 7 days. **(C)** CD25 expression was determined in cells cultured as in (B). MFI, mean fluorescence intensity. **(D)** Representative contour plots of cytokine production by human *TRIB2*-deficient naïve CD4$^+$ T cells as described in Figure 3D. **(E and F)** Human naïve CD8$^+$ T cells were cultured with plate-bound anti-CD3/anti-CD28 (5 µg/ml) in the presence of indicated FANA-ASO for 5 days and analyzed for CD25 mean fluorescence intensity, MFI (E) and cytokine production after restimulation with PMA and Ionomycin (F). **(G and H)** Cytokine production (G) and CD25 expression (H) of purified human naïve CD4$^+$ T cells that were transduced with GFP-containing empty vector or GFP-containing *TRIB2*-overexpressing (OE) lentivirus and cultured for 5 days. For cytokine assessments, cells were re-stimulated with PMA and ionomycin for 4 hours. All datapoints represent distinct biological replicates. Results are pooled from 2 (B, C, E, F) and 3 experiments (A, G, H). Data were compared by two-tailed, paired *t*-tests (A to C, E to H). *P<0.05, **P≤0.01, ***P≤0.001. ns, not significant.

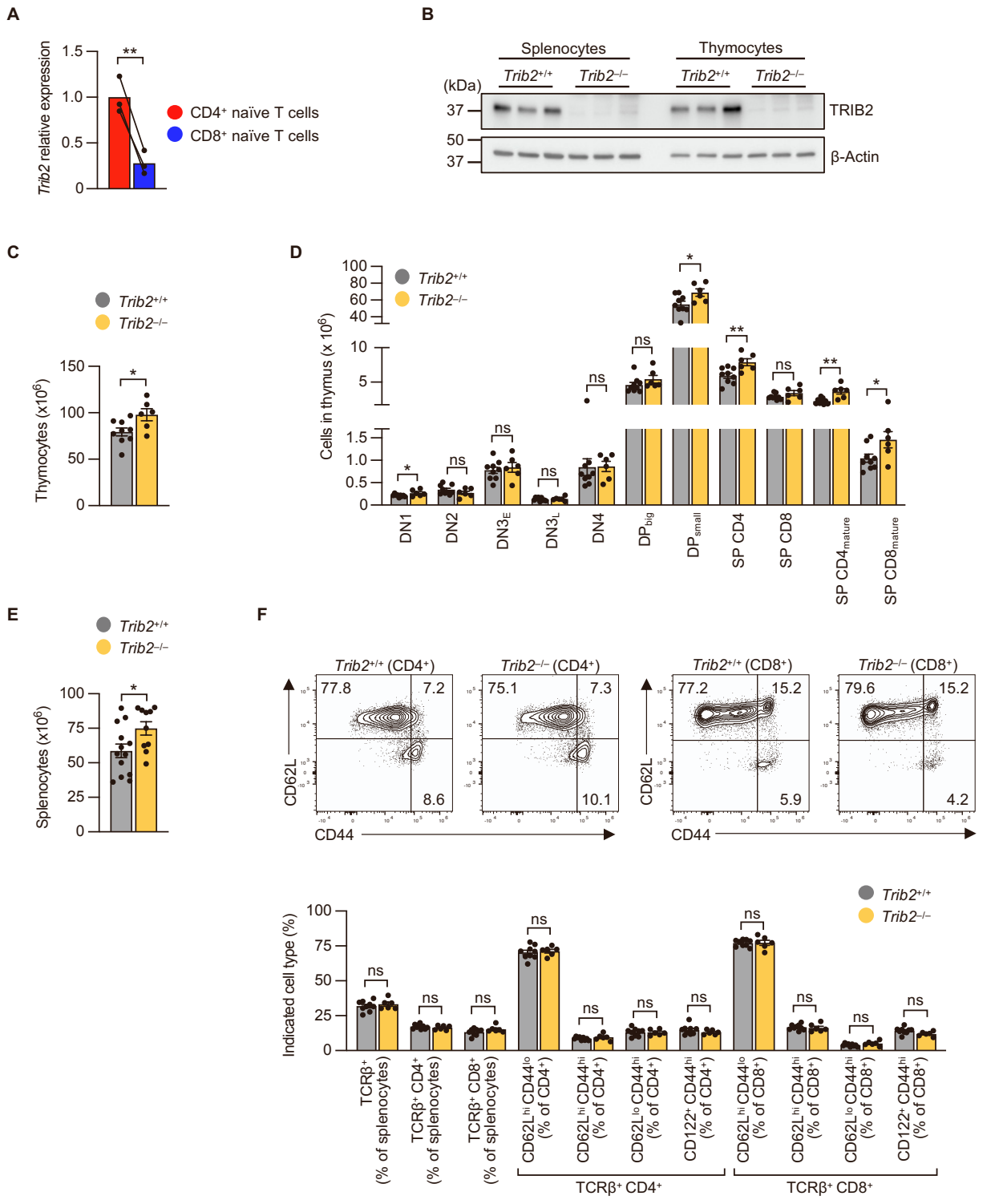

Figure S3, related to Figure 4. Loss of *Trib2* increases the number of T cells irrespective of subset. (A) *Trib2* mRNA expression in purified murine naïve CD4⁺ or CD8⁺ T cells from spleens of wild-type mice as measured by RT-qPCR. **(B)** Immunoblot

of TRIB2 protein levels in total splenocytes or thymocytes from wild-type and *Trib2* knockout mice. **(C)** Thymocyte numbers of wild-type and *Trib2* knockout mice. **(D)** Thymocyte subset numbers in wild-type and *Trib2* knockout mice as measured by cell counts and flow cytometry. DN1 ($CD4^-$ $CD8^-$ $CD44^+$ $CD25^-$), DN2 ($CD4^-$ $CD8^-$ $CD44^+$ $CD25^+$), $DN3_E$ ($CD4^-$ $CD8^-$ $CD44^-$ $CD25^+$ FSC-A^{lo}), $DN3_L$ ($CD4^-$ $CD8^-$ $CD44^-$ $CD25^+$ FSC-A^{hi}), DN4 ($CD4^-$ $CD8^-$ $CD44^-$ $CD25^-$), DP_{big} ($CD4^+$ $CD8^+$ FSC-A^{hi}), DP_{small} ($CD4^+$ $CD8^+$ FSC-A^{lo}), SP CD4 ($CD4^+$ $CD8^-$), SP CD8 ($CD4^-$ $CD8^+$), SP $CD4_{mature}$ ($CD4^+$ $CD8^-$ TCRβ^+ $CD24^-$), SP $CD8_{mature}$ ($CD4^-$ $CD8^+$ TCRβ^+ $CD24^-$). **(E)** Splenocyte numbers of wild-type and *Trib2* knockout mice. **(F)** Proportion of $CD4^+$ and $CD8^+$ T cell populations and their naïve/memory phenotype in splenocytes of wild-type and *Trib2* knockout mice as analyzed by flow cytometry. Results are shown as mean ± SEM (C to F). All datapoints represent distinct biological replicates. Results are from 1 experiment (A), pooled from 2 (C, D, F) or 3 experiments (E). Data were compared by two-tailed, unpaired *t*-tests (A, C to F). $*P<0.05$, $**P\leq0.01$. ns, not significant.

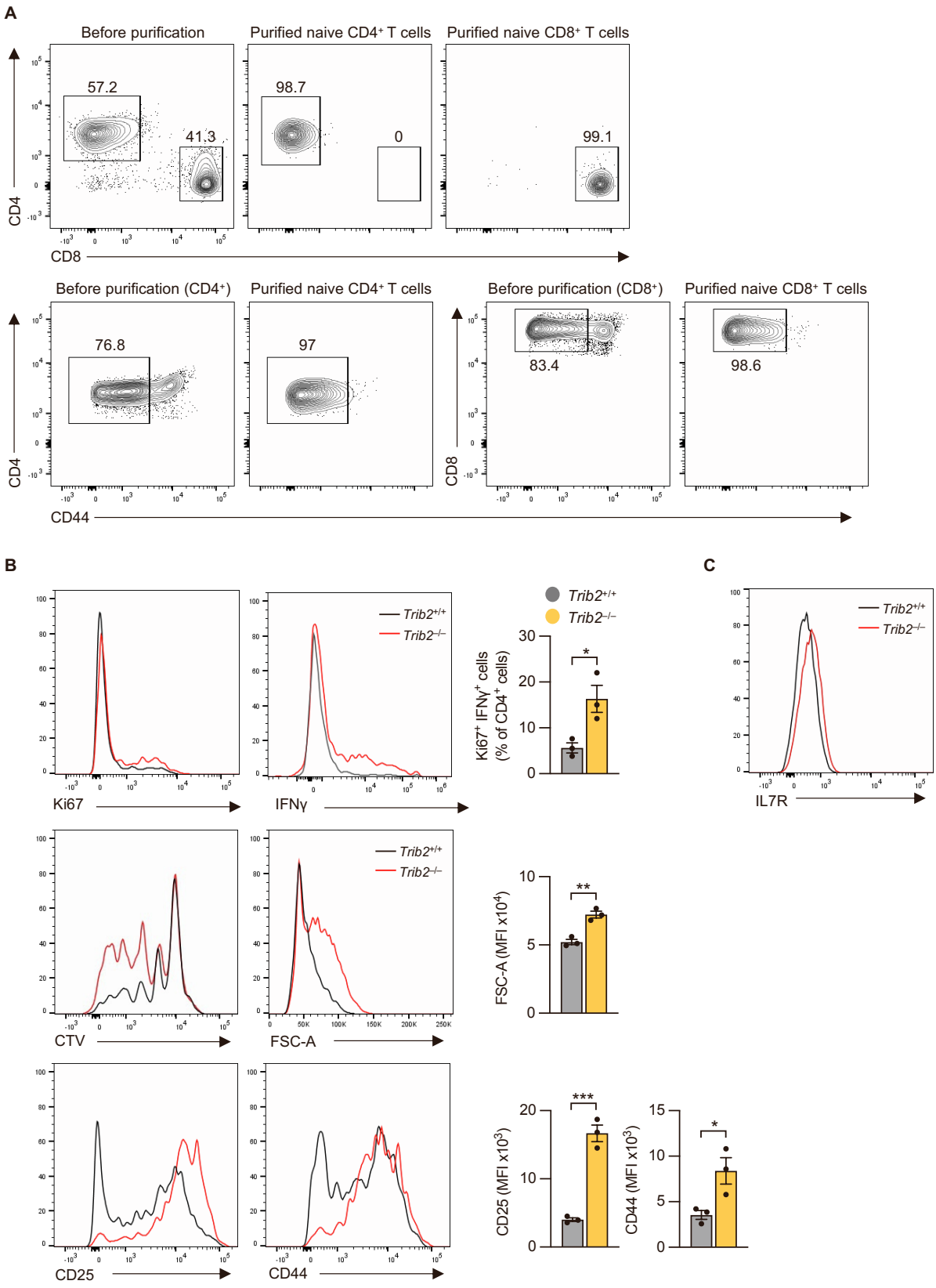
A
Before purification
Purified naive CD4⁺ T cells
Purified naive CD8⁺ T cells
57.2
41.3
98.7
0
99.1
CD4
CD8
Before purification (CD4⁺)
Purified naive CD4⁺ T cells
Before purification (CD8⁺)
Purified naive CD8⁺ T cells
76.8
97
83.4
98.6
CD4
CD8
CD44
B
Trib2+/+
Trib2−/−
Ki67
IFNγ
Ki67⁺ IFNγ⁺ cells (% of CD4⁺ cells)
CTV
FSC-A
FSC-A (MFI x10⁴)
CD25
CD44
CD25 (MFI x10³)
CD44 (MFI x10³)
C
IL7R

Figure S4, related to Figure 4. *Trib2* loss promotes T cell proliferation and activation. (A) Purity of naïve $CD4^+$ or naïve $CD8^+$ T cells from murine spleens before and after cell sorting. Representative contour plots of $CD4^+$ and $CD8^+$ cells (top) and proportion of naïve ($CD62L^{hi}$ $CD44^-$) cells within $CD4^+$ or $CD8^+$ T cells (bottom) as measured by flow cytometry. **(B)** Naïve $CD4^+$ T cells from wild-type and *Trib2* knockout mice were labeled with CTV and cultured with indicated plate-bound anti-CD3/anti-CD28 antibodies (2.5 μg/ml) for 5 days. Representative histograms and quantitation of IFNγ production, Ki67 positivity, CTV dilution, forward scatter (FSC-A), CD25 and CD44 expression. **(C)** IL7R expression in naïve $CD4^+$ T cells from wild-type or *Trib2* knockout mice. Results are shown as mean ± SEM (B). All datapoints represent distinct biological replicates. Results are from 1 experiment (A, B). Data were compared by two-tailed, unpaired *t*-tests (B). $*P<0.05$, $**P\leq0.01$, $***P\leq0.001$.

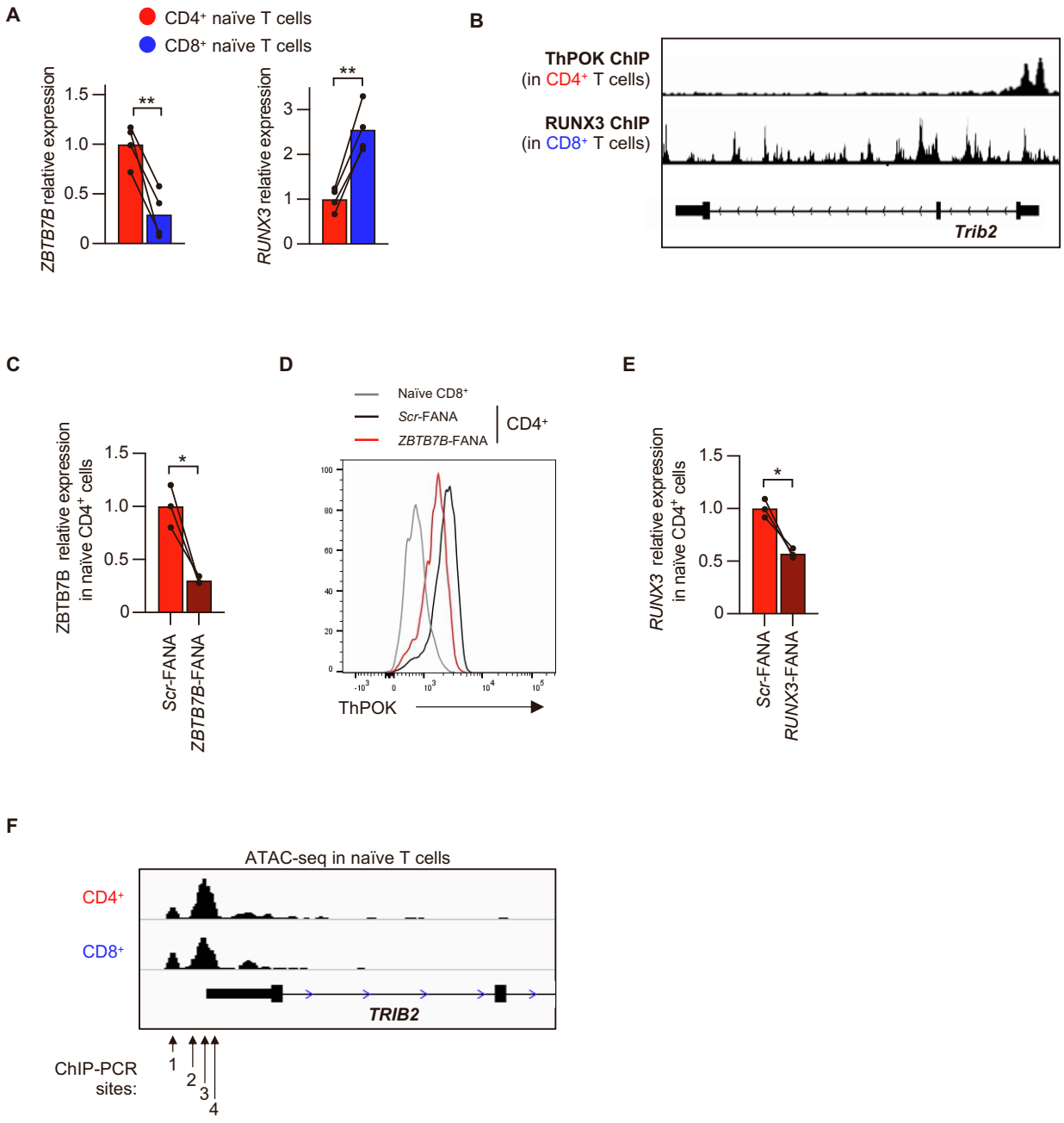

Figure S5, related to Figure 5. ThPOK and RUNX3 regulate *TRIB2* expression. (A) Expression of *ZBTB7B* (ThPOK) and *RUNX3* in purified human naïve CD4⁺ and CD8⁺ T cells as measured by RT-qPCR. **(B)** ThPOK binding in mouse CD4⁺ T cells and RUNX3 binding in mouse CD8⁺ T cells at the *Trib2* locus from published ChIP-seq data: GSE116506 for ThPOK ChIP-seq; GSE50130 for RUNX3 ChIP-seq. **(C and D)** Efficiency of FANA-ASO-mediated *ZBTB7B* (ThPOK) knockdown in purified human naïve CD4⁺ T cells as determined by RT-qPCR (C) or flow cytometry (D). **(E)** Efficiency of FANA-ASO-

mediated *RUNX3* knockdown in purified human naïve $CD4^+$ T cells as determined by RT-qPCR. **(F)** ATAC-seq chromatin accessibility profiles at the *TRIB2* locus of human naïve $CD4^+$ or $CD8^+$ T cells (analyzed from SRA accession code PRJNA478249 and dbGaP accession code phs001187.v1.p1). Putative transcription factor binding sites 1 through 4 are indicated. All datapoints represent distinct biological replicates. Results are from 1 experiment (A), pooled from 2 experiments (C, E). Data were compared by two-tailed, paired *t*-tests (A, C, E). $*P<0.05$, $**P\leq0.01$.

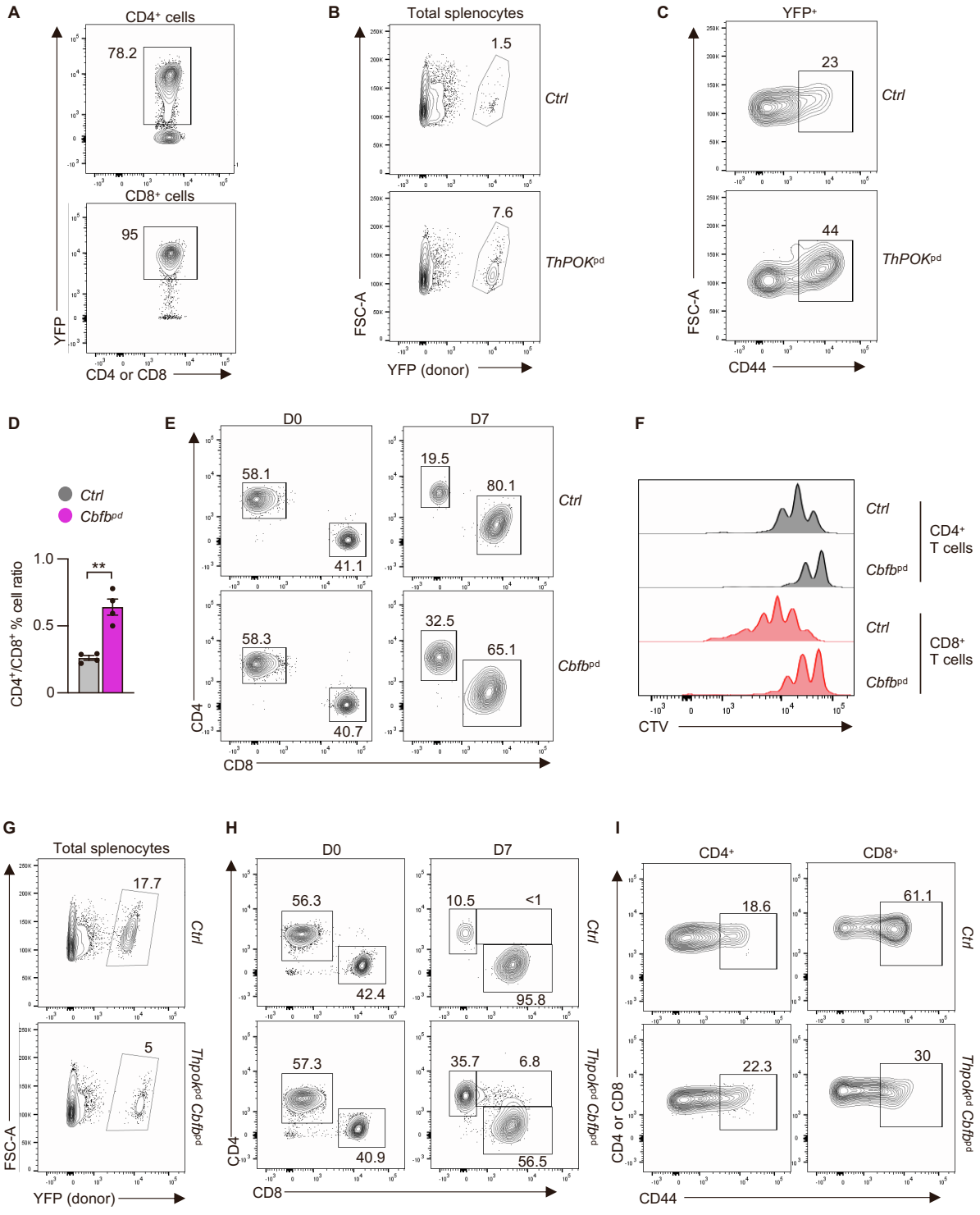

Figure S6, related to Figure 5. ThPOK and RUNX3 regulate lymphopenia-induced proliferation of T cells. (**A**) Deletion efficiency of CD2-Cre recombinase as measured by YFP expression in T cells from murine spleen (originating from the Cre-sensitive

transgene LoxP-Stop cassette-LoxP-YFP). CD2-Cre was used to conditionally knock out *Cbfb* and/or *ThPOK* in peripheral T cells. **(B)** Representative contour plots of splenocytes from lymphopenic mice that were reconstituted with YFP^+ donor cells of *Ctrl* ($CD2\text{-}Cre^+$ $ThPOK^{fl/+}$ *Rosa26*-$YFP^{fl/+}$) or $ThPOK^{pd}$ ($CD2\text{-}Cre^+$ $ThPOK^{fl/fl}$ *Rosa26*-$YFP^{fl/fl}$) mice. Splenocytes were analyzed 7 days post-transfer. **(C)** Representative CD44 contour plots of YFP^+ donor cells. **(D to F)** Characterization of $Cbfb^{pd}$ T cells during lymphopenia. YFP^+ $CD4^+$ $CD44^-$ and YFP^+ $CD8^+$ $CD44^-$ T cells were sorted from *Ctrl* ($CD2\text{-}Cre^+$ $Cbfb^{fl/+}$ *Rosa26*-$YFP^{fl/+}$) and $Cbfb^{pd}$ ($CD2\text{-}Cre^+$ $Cbfb^{fl/fl}$ *Rosa26*-$YFP^{fl/fl}$) mice, respectively (D0). $CD4^+$ and $CD8^+$ T cells were pooled for each genotype, labeled with CTV and adoptively transferred into irradiated wild-type mice. One week later (D7), splenocytes were analyzed by flow cytometry for ratios of $CD4^+$ and $CD8^+$ T cells (D and E) and their CTV dilution (F). **(G to I)** Representative contour plots of donor cell recovery (G), $CD4^+$ and $CD8^+$ T cell subset proportions (H) and CD44 expression (I) after adoptive transfer of $CD2\text{-}Cre^+$ $ThPOK^{fl/+}$ $Cbfb^{fl/+}$ *Rosa26*-$YFP^{fl/+}$ (*Ctrl*) and $CD2\text{-}Cre^+$ $ThpPOK^{fl/fl}$ $Cbfb^{fl/fl}$ *Rosa26*-$YFP^{fl/fl}$ ($Thpok^{pd}$ $Cbfb^{pd}$) T cells in Figure 5J-N. Data are presented as means ± SEM. All datapoints represent distinct biological replicates. Results are representative of 4 experiments (A), or of 2 experiments with 3-4 mice in each group (D). Data were compared by two-tailed, unpaired *t*-test (D). $^{**}P \leq 0.01$.

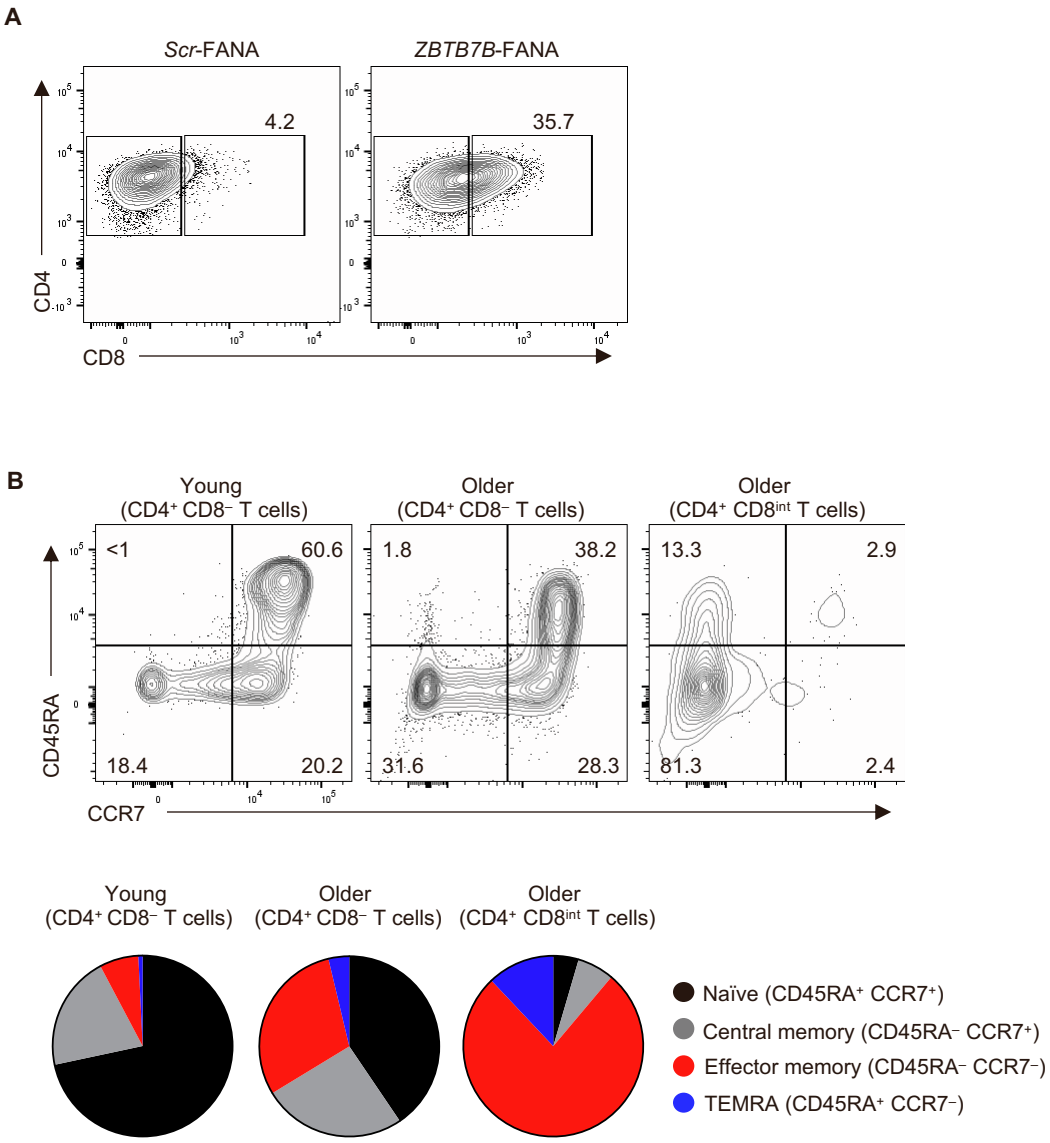

Figure S7, related to Figure 7. Age-related TRIB2 deficiency correlates with effector traits. (A) CD8α expression after *ZBTB7B (*ThPOK) knockdown in purified human naïve $CD4^+$ T cells. Cells were activated with anti-CD3/anti-CD28 Dynabeads at a bead-to-cell ratio of 1:5 in presence of indicated FANA-ASO for 9 days. CD4 and CD8 levels were analyzed by flow cytometry. Contour plots are representative of 3 experiments. **(B)** Phenotype of $CD4^+$ $CD8^{int}$ T cells as assessed by flow cytometry. Representative contour blots (top) and distribution of cell population with indicate differentiation states (bottom).

Name	Forward Primer (5’ – 3’)	Reverse Primer (5’ – 3’)
RT-qPCR primers		
mTrib2	ATACACAGGTCTACCCCTATCAC	ATGCGACAAGTTCGGAGTCTC
mZbtb7b	CCCGAGGATGACCTGATTGG	CCTGCGTCCTGATGGTGAG
mRunx3	CAGGTTCAACGACCTTCGATT	GTGGTAGGTAGCCACTTGGG
mActb	GGCTGTATTCCCCTCCATCG	CCAGTTGGTAACAATGCCATGT
hTRIB2	ATACACAGGTCTACCCTTATCAC	ATGCGACAAGTTCGGAGTCTC
hZBTB7B	GTCCCCAGAGCTACGAACC	AGCTTAGGTAGGCCATCAGGT
hRUNX3	GCGAGGGAAGAGTTTCACCC	TTGATGGCTCGGTGGTAGGT
hACTB	ATGGCCACGGCTGCTTCCAGC	CATGGTGGTGCCGCCAGACAG
ChIP-PCR primers		
Site1	AATGGAGAGGAGGATGTCGG	TCATGTTCCTGGCGCTTTTC
Site2	GAAAAGCGCCAGGAACATGA	GTGAAATATCCTTCCGCGGC
Site3	TCACTTTGTTTACCTCCCCG	CGCCCATCAATCAGCCCC
Site4	GGAGGCTCCGTGGAAATGT	GGCGAGGCGGTATTAATAGTTAC

Table S1, related to Key Resources Table. Primer sequences.